

Superfluid-Insulator Transition of Interacting Multi-Component Bosons — Gutzwiller Variational and Quantum Monte Carlo Study —

Yukitoshi MOTOME and Masatoshi IMADA

*Institute for Solid State Physics, University of Tokyo,
Roppongi 7-22-1, Minato-ku, Tokyo 106*

(Received February 14, 1996)

Various types of superfluid-insulator transitions are investigated for two-component lattice boson systems in two dimensions with on-site hard-core repulsion and the component-dependent intersite interaction. The mean-field phase diagram is obtained by the Gutzwiller-type variational technique in the plane of filling and interaction parameters. Various ground-state properties are also studied by the quantum Monte Carlo method. Our model exhibits two types of diagonal long-range orders; the density order around the density $n = 1/2$ and the Ising-type component order near $n = 1$. The quantum Monte Carlo results for the transitions from the superfluid state to these two ordered states show marked contrast with the Gutzwiller results. Namely, although they are both accompanied by phase separation into commensurate ($n = 1/2$ or $n = 1$) and incommensurate density phases, these transitions are both continuous. The continuous growth of the component correlation severely suppresses the superfluidity as well as the inverse of the effective mass in the critical region of the component order transition in contrast to the persistence of the superfluidity in the density-ordered state. We propose a mechanism of the mass enhancement observed even far from the Mott insulating filling $n = 1$, when the Ising-type component order persists into $n \neq 1$. Possible relevance of this type of mass enhancement in other systems is also discussed.

KEYWORDS: superfluid-insulator transition, Mott transition, two-component boson system, component long-range order, Ising exchange, phase separation, strong mass enhancement

§1. Introduction

Recently, the scaling theory of the metal-insulator transition has been proposed¹⁾, where the critical nature of the transition depends on characters of both of the insulating and the metallic states. An origin of the difference in characters is due to a variety of the spin degrees of freedom such as the antiferromagnetic long-range order or the spin excitation gap. These differences cause various different types of metal-insulator transitions. This scaling theory has been combined with numerical results of the two-dimensional Hubbard model leading to the finding of a new universality class in the Mott transitions. Numerical calculations show following singular properties: (1) In the metallic state, the charge susceptibility χ_c is inversely proportional to the hole density $\delta = 1 - n$ near the Mott transition at the commensurate density $n = 1$ ²⁾. This singularity has been interpreted as the effective mass divergence. (2) In the insulating state, the localization length is proportional to $\Delta^{-1/4}$, where $\Delta = \mu - \mu_c$ ³⁾. Here, μ is the chemical potential and μ_c is the critical value of μ at the transition. In terms of the scaling theory, these singularities lead to a new universality class of the metal-insulator transition with the dynamical exponent $z = 1/\nu = 4$ where ν is the correlation length exponent.

In strongly correlated boson systems, the scaling theory for the superfluid-insulator transition has also been proposed⁴⁾. Predictions from this theory have been tested favorably by many numerical works^{5, 6)}. However, bosons are usually considered as single-component objects, compared with two spin components, up and down, in fermion systems. The dynamical exponent z is believed to be two at the transition between the Mott insulator and the superfluid. Because of the absence of component degrees of freedom, the superfluid-insulator transition in the single-component case is indeed the same as the transition of fermions from metal to the band insulator in the sense of the universality class.

Recently, in the exact diagonalization of clusters, the divergence of the density susceptibility has been suggested in the two-dimensional boson t - J model⁷⁾ where the system consists of interacting two-component bosons as we define later. In this model, each boson has a component index $+$ or $-$ as in the spin, up or down, of fermion systems. Small clusters show qualitatively different behavior between the density and the component susceptibility in the critical region near the Mott insulating state at $n = 1$. Especially, a remarkable result is a critical enhancement of the density susceptibility. This suggests the possible existence of a novel universality class of the superfluid-insulator transition in the multi-component boson systems, similarly to the metal-insulator transition in fermion systems. The boson t - J_Z model, which is the boson t - J model in the absence of the component exchange interaction, $J_{XY} = 0$, has also been investigated⁷⁾. This model exhibits a continuous transition to the component-ordered state at a finite hole concentration. Although critical exponents have not been quantitatively estimated, the chemical potential μ in the critical region indicates different aspects from that in the transition with $z = 1/\nu = 2$. More specifically, the divergence of the

density susceptibility at the transition has been suggested. In this previous study, the superfluidity of the quantum liquid state has not been explicitly investigated.

One of the purposes of the present work is to study the transition to the component-ordered state in two-component boson systems in more detail. We calculate the superfluid density to identify the critical point of the superfluid-insulator transition. Through the study of the component correlation around this transition, we identify the nature of the insulating state. The critical properties at this transition are also investigated in detail.

The second purpose is to clarify possible variety of the universality class even within the boson systems, where the transition is between the superfluid and insulator. Our models exhibit two types of insulating states, one with and the other without the component order. Comparison of critical properties near the both transitions into these two insulating states helps us to understand roles of component symmetry breaking on the superfluid-insulator transition.

The third purpose of this paper is to study the interplay of the component order transition at an incommensurate density, $n \neq 1$, and the transition to the Mott insulator at $n = 1$. Our models show the transition to the component-ordered state at a finite hole density accompanied by the strong mass enhancement. We propose the mechanism of this remarkable enhancement of the effective mass near the component order transition into Ising-type order. This mechanism of strong mass enhancement may be rather different from that of the mass divergence at $n = 1$. The persistence of the component order at $n \neq 1$ and the mass enhancement are both crucially related with the Ising-like nature of the component order.

These studies may help us to gain more insight from a slightly different viewpoint on the origin and the mechanism of the novel universality class with $z = 1/\nu = 4$ at the Mott transition seen in the two-dimensional Hubbard model. This is a first step to discuss the universal aspects of various types of the Mott transitions beyond the statistics of particles. One advantage of studying boson systems is that they can relatively easily be treated by numerical approaches, because, for example, the negative sign difficulty in the quantum Monte Carlo method does not appear in many cases.

The outline of this paper is as follows. In §2, our model is introduced. Our model includes many models which have been investigated before. We briefly review these previous studies. Methods of our calculation are explained briefly in §3. We use two methods in the present study. One is the Gutzwiller-type variational technique, which is the mean field type approach, and the other is the quantum Monte Carlo method with the world-line algorithm. We show our results in §4. In contradiction to the mean field prediction, our model exhibits a strong mass enhancement when it undergoes the continuous transition into the component-ordered insulator at an incommensurate density. In §5, comparing this with other types of superfluid-insulator transitions, we propose a relevant mechanism for our results. Relevance of this type of mass enhancement to other problems is discussed. Finally, §6 is devoted to the summary.

§2. Model

In this work, we consider the two-component boson system on a two-dimensional square lattice. Each boson has a component index $s = +$ or $-$, and both have hard-core repulsion which restricts the Hilbert space by excluding the double occupancy of any bosons at the same site. The Hamiltonian is given by

$$\mathcal{H} = \sum_{\langle ij \rangle} \mathcal{H}_{ij} \quad (2.1)$$

$$= \sum_{\langle ij \rangle} \left[-t \sum_{s=+,-} \left(\tilde{a}_{i,s}^\dagger \tilde{a}_{j,s} + \text{h.c.} \right) + V n_i n_j + W S_i^z S_j^z \right], \quad (2.2)$$

where

$$\tilde{a}_i^\dagger = a_i^\dagger (1 - a_i^\dagger a_i) \quad (2.3)$$

with a_i^\dagger (a_i) being a boson creation (annihilation) operator for site i . Summations on $\langle ij \rangle$ are over the nearest neighbor pairs. In (2.1), the number and spin operators are defined as

$$n_i = \sum_{s=+,-} a_{i,s}^\dagger a_{i,s}, \quad (2.4)$$

$$S_i^z = \frac{1}{2} (a_{i,+}^\dagger a_{i,+} - a_{i,-}^\dagger a_{i,-}). \quad (2.5)$$

We note that any type of the diagonal interaction between the nearest neighbor sites can be realized by choosing proper V and W . This model (2.1) includes, as limiting cases, various models already investigated before: (a) The simplest case with $V/t = 0$ and $W/t = 0$ corresponds to the one-component boson Hubbard model at $U/t \rightarrow \infty$, where U is the on-site interaction⁸⁾. In this case, the superfluid state is realized for $0 < n < 1$ and the Mott transition takes place at $n = 1$. (b) The case with $V/t \neq 0$ and $W/t = 0$ is called the extended boson Hubbard model at $U/t \rightarrow \infty$ with the nearest-neighbor repulsive interaction⁹⁾. This model is known to exhibit the density long-range order around $n = 1/2$ for large values of V/t . (c) The case with $V/t = 0$ and $W/t \neq 0$ is the same model as the boson t - J_Z model with $J_Z = W$ ⁷⁾, where the insulating state at $n = 1$ has the component long-range order of the Ising type. Previous study in this case⁷⁾ has shown that the continuous transition to the component-ordered state occurs at a finite hole concentration $\delta = \delta_c$.

From these previous results in the limiting cases, our model (2.1) is expected to have two types of ordered states. One is the density-ordered state and the other is the component-ordered one. The former should take place near the density-ordered insulator at $n = 1/2$ for large values of V/t . In the case with $W/t \neq 0$, this state may have the component order because of the effective Ising coupling between the next nearest neighbor sites derived from the second order perturbation

in t/V . The latter, the component-ordered state, should occur near $n = 1$. The nearest neighbor repulsion V may work to decrease a tendency for the component order away from $n = 1$. Therefore, for large values of V/t , we expect that the critical hole density δ_c approaches zero.

§3. Methods

3.1 Gutzwiller projection technique

Gutzwiller projection technique was originally devised for the fermion Hubbard model¹⁰⁾. This technique has been applied also to strongly correlated boson systems¹¹⁾. Commutation relations between the boson operators decouple the Gutzwiller wave function into a site diagonal form so that the energy can be exactly estimated quite easily in contrast to the fermion case where the fermion determinant has to be estimated by some types of approximations¹²⁾ or statistical sampling methods¹³⁾. In addition, because we consider hard-core bosons, there is no Gutzwiller variational parameter which controls the ratio of the double occupancy. For the single-component system with hard-core constraint, the Gutzwiller function is explicitly given by¹¹⁾

$$|\Psi\rangle = \prod_i |\phi_i\rangle, \quad (3.6)$$

with

$$|\phi_i\rangle = (1 - n)^{\frac{1}{2}} |0\rangle_i + n^{\frac{1}{2}} |1\rangle_i \quad (3.7)$$

where $|0(1)\rangle_i$ represents an unoccupied (occupied) state at site i . The superfluid order parameter evaluated by this wave function (3.6) is

$$\Delta_s \equiv \frac{1}{L^2} \sum_i \langle \Psi | a_i^\dagger | \Psi \rangle^2 = n(1 - n), \quad (3.8)$$

therefore, this Gutzwiller state shows the superfluidity except for $n = 0$ or 1 .

Here, we extend this technique to describe ordered states. For the model (2.1) on a bipartite lattice, we may expect the symmetry breaking, such as the density order or the component order. To allow these orderings, we extend the Gutzwiller wave function (3.6) in the form as

$$|\Psi\rangle = \prod_{i \in A} |\phi_i^A\rangle \prod_{j \in B} |\phi_j^B\rangle, \quad (3.9)$$

where $A(B)$ represents $A(B)$ -sublattice and

$$|\phi^A\rangle = (1 - \zeta)^{\frac{1}{2}} |0\rangle + \lambda^{\frac{1}{2}} |+\rangle + (\zeta - \lambda)^{\frac{1}{2}} |-\rangle \quad (3.10)$$

$$\begin{aligned} |\phi^B\rangle &= (1 - 2n + \zeta)^{\frac{1}{2}} |0\rangle \\ &+ (n - \lambda)^{\frac{1}{2}} |+\rangle + (n - \zeta + \lambda)^{\frac{1}{2}} |-\rangle \end{aligned} \quad (3.11)$$

with two variational parameters λ and ζ . Here, $|+(-)\rangle$ represents an occupied state with a $+(-)$ component boson.

This extended Gutzwiller function (3.9) represents various states according to the values of λ and ζ as follows: (i) When $\lambda = n/2$ and $\zeta = n$, (3.9) is ascribed to the single component case (3.6) because $|\phi^A\rangle = |\phi^B\rangle$. Therefore, for $0 < n < 1$, it represents the superfluid state without any ordering of density or spin. (ii) In the case of $\lambda \neq n/2$ and $\zeta = n$, we have the component-ordered state of the Ising type, which is characterized by

$$\langle S_{i \in A}^z \rangle = -\langle S_{j \in B}^z \rangle \neq 0, \quad \langle n_{i \in A} \rangle = \langle n_{j \in B} \rangle = n. \quad (3.12)$$

(iii) In the case with $\lambda = \zeta/2$ and $\zeta \neq n$, the density-ordered state appears, that is,

$$\begin{aligned} \langle n_{i \in A} \rangle - n &= -(\langle n_{j \in B} \rangle - n) \neq 0, \\ \langle S_{i \in A}^z \rangle &= \langle S_{j \in B}^z \rangle = 0. \end{aligned} \quad (3.13)$$

(iv) For other values of λ and ζ , we have the mixed state, which is the coexistence of the component and density order defined by

$$\langle S_{i \in A}^z \rangle \neq \langle S_{j \in B}^z \rangle, \quad \langle n_{i \in A} \rangle \neq \langle n_{j \in B} \rangle. \quad (3.14)$$

In all these states, the superfluid order parameter Δ_s has a finite value except for $n = 0$ or 1 .

We determine the values of λ and ζ to minimize the expectation value of the Hamiltonian (2.1). From this minimization, we draw the Gutzwiller phase diagram. The mean field picture on the transitions to the ordered states is discussed in 4.1.

3.2 Quantum Monte Carlo technique

To get more accurate and unbiased results on various physical quantities in the ground state, we investigate by the quantum Monte Carlo (QMC) method with the world-line algorithm. The technique which we choose is a standard one¹⁴⁾. First, we rewrite the partition function using the Suzuki-Trotter formula,

$$Z \equiv e^{-\beta \mathcal{H}} \quad (3.15)$$

$$= \lim_{M \rightarrow \infty} \left(e^{-\Delta \tau \mathcal{H}} \right)^M \quad (3.16)$$

$$= \lim_{M \rightarrow \infty} \left[e^{-\Delta \tau (\mathcal{H}_X^{\text{odd}} + \mathcal{H}_Y^{\text{odd}} + \mathcal{H}_X^{\text{even}} + \mathcal{H}_Y^{\text{even}})} \right]^M, \quad (3.17)$$

where $\beta = T^{-1}$ (we set $\hbar = k_B = 1$) is the inverse temperature and $M = \beta/\Delta\tau$ is called the Trotter number. In (3.17), we make the checkerboard decomposition, where $\mathcal{H}_{X(Y)}^{\text{odd(even)}}$ represents the Hamiltonian (2.1) for odd(even) bonds in the $x(y)$ direction. These procedures map the original quantum problem in two dimensions into the classical one in $(2+1)$ dimensional space composed of plaquettes on which world lines lie. Each Monte Carlo update is accepted by the ratio of the probability

$$\begin{aligned} &P(n_i(\tau_l), n_j(\tau_l); n_i(\tau_{l+1}), n_j(\tau_{l+1})) \\ &= \langle n_i(\tau_l) n_j(\tau_l) | e^{-\Delta \tau \mathcal{H}_{ij}} | n_i(\tau_{l+1}) n_j(\tau_{l+1}) \rangle \end{aligned} \quad (3.18)$$

between after and before the change in configurations on each plaquette. Here, $\tau_l = l\Delta\tau$ ($l = 0, 1, \dots, 4M$) is the position in the imaginary time direction.

The calculation is done for the system size $L \times L$, $L = 4, 6$ and 8 with $\beta = 10$ which is low enough temperature to investigate the ground-state properties for most of our purposes¹⁶⁾. We take periodic boundary conditions in both spatial and temporal directions. Our calculation is done in a canonical ensemble, that is, the density n is fixed in Monte Carlo steps. The systematic errors caused by finite M are proportional to $(\Delta\tau)^2$ in the lowest order. The extrapolation to $M \rightarrow \infty$ has been done by using several values of M between 40 and 100 for each L , n and β . In the actual calculation, typically 10000-20000 sequence of configurations are discarded for the thermalization to realize the statistical equilibrium. We actually take 100000-1000000 samples for each measurement depending on the situation.

In the calculation, we take two local updates and three global updates¹⁴⁾. The latter global updates are typically illustrated in Figure 1. Figure 1 (a) and (b) are temporal global flips, which are uniform moves or exchanges of straight world lines. The latter one in Figure 1 (b) can exchange different component bosons, which is important near $n = 1$ because of the low acceptance ratio of local updates caused by the growth of the component order. The last one in Figure 1 (c) is a spatial global flip which reconnect same component world lines in every other plaquette. This updating procedure can change the winding number, therefore, it is important for estimates of global physical quantities like the superfluid density.

§4. Results

4.1 The Gutzwiller phase diagram and the mean field analysis on the transitions to the ordered states

Applying the procedure explained in §3.1, we determine the Gutzwiller phase diagram. The results are depicted in Figure 2.

When $W/t = 0$, Figure 2 (a), which is equivalent to the single-component case, shows the density-ordered state around $n = 1/2$ for large values of V/t . In this case, the expectation value of the Hamiltonian (2.1) with the Gutzwiller-type wave function (3.9) is given by

$$\begin{aligned} \langle \Psi | \mathcal{H}_{ij} | \Psi \rangle = & -2t\zeta^{\frac{1}{2}}(2n - \zeta)^{\frac{1}{2}}(1 - \zeta)^{\frac{1}{2}}(1 - 2n + \zeta)^{\frac{1}{2}} \\ & + V\zeta(2n - \zeta). \end{aligned} \quad (4.19)$$

The minimization of (4.19) with the variational parameter ζ gives the threshold density for the density long-range order as

$$n_c = \frac{1}{2} \left[1 \pm \sqrt{\frac{v-1}{v+1}} \right], \quad (4.20)$$

where $v \equiv V/2t$. This result agrees with the previous result by another type of mean field analysis for the extended boson Hubbard model⁹⁾. At $n = 1/2$, the insulating state with the density order

Fig. 1. Examples of the global flip in the QMC calculation. In all figures, the horizontal direction is a spatial one and the vertical direction is the temporal one. All gray squares are plaquettes in the checkerboard decomposition (3.17), Solid and dotted lines illustrate the world lines. Filled and open circles are bosons of the component $+$ and $-$, respectively. (a) illustrates a uniform move of a straight world line, (b) is for an exchange of straight world lines of different component and (c) shows a spatial global flip which changes the winding number.

appears for $v > 1.0$. This is indicated by a kink of the ground state energy as the function of n . In the hatched region in Figure 2 with $n \neq 1/2$, the superfluidity and the density order coexist in uniform phase. These features on the density-ordered state persist even for $W/t \neq 0$, except for the mixed state as explained below.

When W/t is switched on, a phase-separated region appears near $n = 1$ as shown in Figure 2. As explained below, this is determined by a convex region in the curve of the ground state energy as the function of n . As a simple example, we consider the $V/t = 0$ case. The expectation value of (2.1) at $V/t = 0$ is given by

$$\begin{aligned} \langle \Psi | \mathcal{H}_{ij} | \Psi \rangle = & -4t(1-n)\lambda^{\frac{1}{2}}(n-\lambda)^{\frac{1}{2}} \\ & + \frac{W}{4}(4n\lambda - 4\lambda^2 - n^2). \end{aligned} \quad (4.21)$$

From the minimization of (4.21) with λ gives the component-ordered state for

$$0 \leq \delta \leq \delta^* = \frac{w}{w+1}, \quad (4.22)$$

where $w \equiv W/4t$. However, more careful analysis shows that this does not really happen as follows. Because the ground state energy obtained by the minimization of (4.21) has a convex region adjacent to $n = 1$ as the function of n , a phase separation occurs into two states, one at

Fig. 2. The Gutzwiller phase diagrams. Figures (a),(b),(c) and (d) correspond to $W/t = 0.0, 0.5, 1.0$, and 1.5 , respectively. Hatched areas are for the density-ordered state with superfluidity, gray areas are the phase-separation into the component-ordered phase and the superfluid phase, and black areas are for the coexistence of the density and component order, respectively. The straight lines at $n = 1/2$ and $V/t > 2.0$ represent the insulating states with the density order. The superfluidity is realized in all the other regions except for the cases with $n = 1/2$ and $V/t > 2.0$, $n = 0$ and 1 .

$n = 1$ and the other at $n \neq 1$. The value of critical hole density δ_c for the phase separation line is determined by drawing the tangent to the ground-state energy curve from the end point of this curve at $n = 1$ in the plane of filling and energy. In the special case with $V/t = 0$ which we consider here, this critical point δ_c is given as

$$\delta_c = \sqrt{\frac{2w}{w+4}}. \quad (4.23)$$

For all values of W/t , δ_c is larger than δ^* . Therefore, when $\delta \rightarrow 0$, what happens in practice is the phase separation for $0 \leq \delta \leq \delta_c$. There, we have the coexistence of the superfluid state without the component long-range order at $\delta = \delta_c$ and the component-ordered state of the Ising type at $n = 1$. In more general, the value of δ_c for $V/t \neq 0$ is determined numerically and δ_c is found to be larger than δ^* for all values of V/t and W/t . As shown in Figure 2, the larger V/t gives the narrower region of this phase separation. The mixed state defined in §3.1 occurs in the region beyond the

intersecting point of curves for n_c and δ_c , as shown in Figure 2 (c) and (d). There, large values of V/t and W/t cause complex orderings, however, this mixed state is beyond our scope of the present study.

These mean field analyses suggest the following pictures of the critical properties at the transition into the phase-separated region near $n = 1$. Here, we discuss behavior of the superfluid order parameter Δ_s and the correlation length ξ of the component correlation. The correlation length ξ is defined from

$$\langle \Psi | S_i^z S_j^z | \Psi \rangle \sim (-)^{|R_{ij}|} \exp \left(-\frac{|\vec{r}_{ij}|}{\xi} \right), \quad (4.24)$$

where R_{ij} is the Manhattan distance between the site i and j . By definition, ξ diverges in the component-ordered state. The above Gutzwiller results suggest following behavior of Δ_s and ξ^{-1} , as schematically depicted in Figure 3. As shown in Figure 3 (a), the phase separation into the superfluid state at $\delta = \delta_c$ and the insulator at $n = 1$ predicts

$$\Delta_s = \frac{\delta}{\delta_c} \Delta_s(\delta = \delta_c) \quad (4.25)$$

for $0 \leq \delta \leq \delta_c$. Moreover, the absence of the component long-range order at $\delta = \delta_c$ leads to a jump of ξ^{-1} as shown in Figure 3 (b). For $0 \leq \delta < \delta_c$, ξ diverges because the Ising-ordered insulator at $n = 1$ coexists with the superfluid state at $\delta = \delta_c$ in this phase separated region. Therefore, this mean field analysis shows that this transition at $\delta = \delta_c$ is a discontinuous one as is usual with the phase separation.

4.2 QMC results

We calculate various physical quantities by the QMC method for two sets of parameters. One is the case with $V/t = 2$ and $W/t = 1$, and the other is the case with $V/t = 4$ and $W/t = 1$. For both cases, we change the density n from 0 to 1. The definitions of physical quantities are the following. The ground state energy per site is given by

$$E_g = \frac{1}{L^2} \langle \mathcal{H} \rangle. \quad (4.26)$$

The bracket defines the canonical ensemble average. The equal-time correlation functions are defined as

$$N(\vec{k}) = \frac{1}{L^2} \sum_{i,j} e^{i\vec{k} \cdot \vec{r}_{ij}} \langle n_i n_j \rangle, \quad (4.27)$$

$$S(\vec{k}) = \frac{1}{L^2} \sum_{i,j} e^{i\vec{k} \cdot \vec{r}_{ij}} \langle S_i^z S_j^z \rangle, \quad (4.28)$$

for the density and the component degrees of freedom, respectively. The superfluid density which measures the stiffness under the twist of the boundary condition is defined as¹⁵⁾,

$$\rho_s = \frac{1}{4\beta} \langle \vec{W}^2 \rangle, \quad (4.29)$$

Fig. 3. Critical behaviors in the transition to the phase-separated region near $n = 1$ suggested from the mean field analysis. (a) is for behavior of the superfluid order parameter and (b) illustrates the inverse correlation length of the component correlation. Gray areas show the phase-separated region, as in Figure 2.

where

$$\vec{W} = \frac{1}{L} \sum_{i=1}^{nL^2} [\vec{r}_i(\beta) - \vec{r}_i(0)] \quad (4.30)$$

is the winding number with $\vec{r}_i(\tau)$ being the position of the i -th boson in $(2 + 1)$ dimensions. A relation between the superfluid density ρ_s and the superfluid order parameter Δ_s should be noted. By definition, if the one-particle wave function extends over the whole system, ρ_s has a finite value. On the other hand, because Δ_s is an order parameter for the superfluidity, it has a non-zero value only in the superfluid state. Therefore, ρ_s and Δ_s may in general be different. For example, in the free boson system in two dimensions, we have $\rho_s \neq 0$ but $\Delta_s = 0$. However, in the interacting boson systems, because the ground state except for the insulating state should be superfluid, we may regard a state with finite ρ_s as a superfluid state with finite Δ_s in the present work.

First, the ground state energy as the function of n is shown in Figure 4 for both cases. Both data exhibit phase-separated regions near $n = 1$, as in the Gutzwiller results. These regions are narrower than those in Figure 2 presumably because of quantum fluctuations. For the latter case with $V/t = 4$, however, another convex region is found around $n = 1/2$. This indicates phase

separation which does not exist in the results of the mean field level in §4.1. In the QMC results, the curve of the ground state energy has a kink at $n = 1/2$ as found in the Gutzwiller result, which indicates that the insulating state with a finite energy gap is realized at $n = 1/2$. Therefore, this new phase separated region is composed of the insulating state at $n = 1/2$ and the state at $n \neq 1/2$ in the hatched area in Figure 4 (b). All the phase-separated regions in Figure 4 are determined from the fitting of the ground-state energy data by the appropriate polynomial function of n .

Next, other physical quantities are shown in Figure 5 and 6. In both cases, we find the component long-range order in the phase-separated regions near $n = 1$ from Figure 5 (a), (b) and 6 (c), (d). Especially, from Figure 5 (b) and 6 (d), the component correlations show continuous growth near the phase separation. In addition, incommensurate peaks are obtained in the component correlation function in these critical regions for $V/t \neq 0$ as shown in Figure 7. In the phase-separated region, the component correlation has commensurate peaks at $\vec{k} = \vec{Q} \equiv (\pi, \pi)$.

For the latter case with $V/t = 4$, we find the density long-range order in the other phase-separated area around $n = 1/2$ from Figure 6 (a) and (b). Similarly to the case of the component order, the density correlation grows continuously in the critical region as in Figure 6 (b). However, we find only the commensurate peaks at $\vec{k} = \vec{Q} \equiv (\pi, \pi)$ in the density correlation function for all values of the density.

It should be noted that the phase-separated region with the density order may have a subtle problem. When $n = 1/2$ and $W/t \neq 0$, the second order perturbation in terms of t/V gives antiferromagnetic Ising coupling between next nearest neighbor pairs in the order of $(W/2t^2) / [(3V)^2 - (W/4)^2]$. Therefore, one might expect that some component order appears with the density order in the ground state at $n = 1/2$ for large V/t ¹⁷⁾. Our results show no numerical evidence of this type of component order as in Figure 6 (c). However, the energy scale for such a component order can be very low, $\ll (W/2t^2) / [(3V)^2 - (W/4)^2] \sim 3.5 \times 10^{-3}$ for the present case with $V/t = 4$ and $W/t = 1$, if it exists, because the frustration may suppress the ordering temperature. All our simulations are done at $\beta = 10$, which may be too high to find this type of component order. Therefore, the density-ordered state which appears in our result should be considered basically as the ground state of the single-component system, although whether the component order is realized or not in the true ground state is not clear as it stands.

Though both of the ordered phases are accompanied by phase separation, ρ_s behaves qualitatively different in each case. In the transition to the phase-separated region with the density long-range order, ρ_s has a finite value, as shown in Figure 6 (e). When $n \rightarrow 1/2$, ρ_s goes to zero continuously. In contrast to this, in the critical region of the component order transition, ρ_s is strongly and continuously reduced, as shown in Figure 5 (c) and 6 (e). In the phase-separated region, ρ_s is always zero within the numerical errorbars.

The observed correlation functions and the superfluid density suggest that the both transitions to

Fig. 4. QMC results of the ground state energy as the function of the density n . (a) is for the case with $V/t = 2$ and $W/t = 1$, and (b) is for $V/t = 4$ and $W/t = 1$. Symbols are circles for $L = 4$, squares for $L = 6$ and triangles for $L = 8$. The gray areas represent the phase-separated regions determined by the convex regions of the ground-state energy curve. The hatched area in (b) is another phase-separated region. The dotted line in each figure is the Gutzwiller result obtained in §4.1 for reference.

Fig. 5. Various physical quantities as the function of the density n for the case with $V/t = 2$ and $W/t = 1$ obtained by the QMC calculation. (a) shows the peak values of the component correlation function $S(\vec{k})$ divided by the system size, (b) is the plot of the inverse of the peak values of $S(\vec{k})$ and (c) is for the superfluid density. Symbols are circles for $L = 4$, squares for $L = 6$ and triangles for $L = 8$. The gray areas represent the phase-separated regions determined by Figure 4.

Fig. 6. Various physical quantities as the function of the density n for the case with $V/t = 4$ and $W/t = 1$ obtained by the QMC calculation. (a) illustrates the density correlation function at $\vec{Q} = (\pi, \pi)$, $N(\vec{Q})$ divided by the system size, (b) shows the inverse of $N(\vec{Q})$, (c) is for the peak values of the component correlation function $S(\vec{k})$ divided by the system size, (d) plots the inverse of the peak values of $S(\vec{k})$ and (e) is for the superfluid density. Symbols are circles for $L = 4$, squares for $L = 6$ and triangles for $L = 8$. The gray and hatched areas represent the phase-separated regions determined by Figure 4. 15

Fig. 7. The component correlation function (4.28) for $V/t = 4$ and $W/t = 1$. (a), (b) and (c) are for $n = 46/64, 50/64$ and $54/64$.

the phase-separated regions with the density and component order are continuous in contradiction to the results of the Gutzwiller results in the previous subsection 4.1.

§5. Discussions

We discuss various remarkable aspects of the QMC results in §4.2 with emphasis on the differences from the Gutzwiller results in §4.1. First, QMC results show the phase-separated region with the density long-range order around $n = 1/2$ as well as that with the component order near $n = 1$ in contrast to the absence of the phase separation around $n = 1/2$ in the Gutzwiller results. The neglect of spatial fluctuations in the mean field analysis appears to be the origin of the failure in reproducing the phase separation around $n = 1/2$. This phase separation may be a consequence of the repulsive interaction assumed only for on-site and the nearest neighbor pairs in our model (2.1). It has been suggested that the next nearest neighbor repulsion eliminates this type of phase separation⁹. A more important contradiction to the mean field results is that both transitions into the phase-separated regions with the component and density orders are continuous. As seen in Figure 5 (b) and 6 (b), (d), each correlation length shows continuous divergence toward the transition. Moreover, the component correlation function, (4.28), shows the incommensurate peaks due to the repulsive interaction V . These behaviors are clearly different from the mean field results, as typically shown in Figure 3 (b). The third point, which is the most remarkable, is the sharp contrast in the superfluid density between the transitions to the density- and component-ordered state. The persistence of ρ_s in the phase-separated state with the density order suggests that this state is composed of the density-ordered insulator at $n = 1/2$ and the superfluid state with the density order at the density of the onset of the phase separation. This behavior of ρ_s at the density order transition is similar to the mean field prediction for the phase-separated state near $n = 1$, as shown in Figure 3 (a). In contrast to this, at the onset of the component order transition, ρ_s vanishes within numerical errorbars, simultaneously with the divergence of the correlation length of the Ising-type component order. This is quite different behavior from that in the mean field analysis, as shown in Figure 3 (a). This result suggests that the component order of the Ising type strongly suppresses the superfluidity.

To compare with the above results on the remarkable suppression of ρ_s , we consider a one-component model which also exhibits the phase separation near $n = 1$. Here, we take the Hamiltonian as

$$\mathcal{H} = -t \sum_{\langle ij \rangle} (\tilde{a}_i^\dagger \tilde{a}_j + \text{h.c.}) + V(1 - n) \sum_{\langle ij \rangle} n_i n_j. \quad (5.31)$$

The QMC data of the ground state energy at $V/t = 1$ is plotted against n in Figure 8 (a). We find that the nearest neighbor repulsion proportional to the hole concentration causes a phase separation near $n = 1$. This phase-separated state is composed of the Mott insulator at $n = 1$ and the state at the onset of the phase separation. The result of ρ_s by the QMC calculation is shown in Figure 8

(b). We find a contrasted behavior of ρ_s from that in the component-ordered phase of Figure 5 (c) and 6 (e). Here, ρ_s has a finite value in the phase-separated region and goes to zero continuously when $n \rightarrow 1$. This suggests that in this single-component case, the phase separation near $n = 1$ does not suppress the superfluidity. These results support that the suppression of the superfluidity is caused by the Ising-type component order, not by the commensurability of the insulating state at $n = 1$. Phase separation in single-component systems or with the density order is compatible with the superfluidity.

Fig. 8. QMC data of the ground state energy (a) and the superfluid density (b) for the one-component model (5.31) with $V/t = 1$. Symbols are circles for $L = 4$ and squares for $L = 6$. The gray area represents the phase-separated region.

The remarkable suppression of ρ_s in the component order transition in our QMC results can be interpreted as the strong mass enhancement as explained below. Generally, in strongly correlated systems, if a single-particle description is possible, the superfluid density may be given as

$$\rho_s \propto \frac{n^*}{m^*}, \quad (5.32)$$

where n^* is the carrier concentration and m^* is the effective mass in this single-particle picture. Therefore, there are two scenarios to cause the superfluid-insulator transition; $n^* \rightarrow 0$ or $m^* \rightarrow \infty$. In fermion systems, the same classification applies, if we consider the Drude weight instead of the superfluid density¹⁸⁾. Especially, in the two-dimensional Hubbard model, the effective mass divergence has been indicated in the Mott transition of fermion systems²⁾. In our results, ρ_s is strongly reduced at a finite hole concentration where the component long-range order sets in. The carrier number n^* is apparently finite at the transition. Therefore, the suppression of ρ_s at $\delta = \delta_c$ indicates the strong enhancement of the effective mass at the transition to the component-ordered state of the Ising type. In contrast to this, in the cases of the density order transition and the phase separation in the single-component model, the effective mass is not enhanced near the transition.

Let us discuss the mechanism of this mass enhancement at the transition to the component-ordered phase at $\delta = \delta_c$. As shown above, this mass enhancement is caused by the component order of the Ising type, not by the other orderings commonly seen even in single-component systems. The reason why the component order survives away from $n = 1$ in two dimensions against strong quantum fluctuations appears actually to be due to the Ising-type exchange. The mechanism of the strong mass enhancement is also ascribed to the Ising-like nature of the component order. As an origin of this remarkable phenomena, we propose the hole trapping in the Ising potential, if the Ising order sets in. In the fermion case, the problem of one hole in the Ising background has been intensively studied^{19,20)}. In that case, because hopping of a hole overturns ordered spins, the hole feels a linearly increasing potential, so-called the string potential, with its move. Therefore, the hole is strongly localized by this Ising potential. If the hole hops around a unit plaquette one cycle and a half, the hole can move to the diagonal site without disturbing Ising spins. It may cause a weak delocalization of the hole under the Ising order. The effective transfer to a diagonal site in a unit plaquette in this mechanism is $32t^6/675W^5$ in the sixth order perturbation in terms of t/W . Although it is still not clear whether the hole is ultimately weakly delocalized due to the presence of this mechanism, it is clear that the hole motion is strongly suppressed under the Ising order and hence the inverse effective mass and ρ_s should be strongly reduced. Because the transition to the Ising-ordered state in our model happens at a finite hole density, the analysis of the effective transfer for a single hole doped into the Ising-ordered insulator mentioned above is not straightforwardly applied. However, because the hole density is small at $\delta = \delta_c$, this scenario of the mass enhancement may be essentially correct. As it stands, it is not clear enough whether the mass m^* is strongly enhanced or really diverges at $\delta = \delta_c$ because of the limitation of this numerical analysis. In any case, at least strong enhancement of m^* and ρ_s^{-1} takes place at the transition to the component-ordered state. Furthermore, it should be noted that the continuous growth of the Ising-type component correlation leads to continuous and remarkable reduction of ρ_s and m^{*-1} even at $\delta > \delta_c$. We note this mechanism of the mass enhancement is relevant when

the next nearest neighbor transfer is zero or small. When longer range transfer than the nearest neighbor becomes large, the mass enhancement will be reduced.

In contrast to the situation under the Ising ordering, in the case of the transition to the density-ordered state, bosons can move without feeling the increasing potential like the string potential under the Ising background. Therefore, the effective mass at this transition may not be enhanced. This may be the reason why ρ_s remains large and finite in this transition. Similarly to this, in the one-component case, ρ_s also remains finite because holes can move without feeling the increasing potential at the onset of the phase separation.

The novel mechanism of the strong mass enhancement proposed above, namely, the hole trapping under the Ising-type correlation even at an incommensurate density, is likely to be effective irrespective of the statistics of particles. That is, if a system has Ising-type degrees of freedom and the Ising order survives to an incommensurate density, the transition to the Ising-ordered state should show the same type of continuous mass enhancement if the range of the transfer t is limited. Here, we discuss a possible relevance of this type of mass enhancement in fermion systems. In the two-dimensional single-band Hubbard model, the component order, in more conventional word, the antiferromagnetic order is not numerically observed away from the commensurate density $n = 1$ presumably due to strong quantum fluctuations. When the component (namely, spin or orbital) order is stabilized in two-dimensional electron systems away from the Mott insulator, it also implies that some additional mechanism such as Ising-type anisotropy is necessary to suppress the quantum fluctuation. Our result suggests that the stabilization mechanism by the Ising anisotropy may also be the origin of strong mass enhancement near the component order transition at an incommensurate density $n \neq 1$ in two dimensions as well as in three dimensions. Although the real phase separation is suppressed by the long-range Coulomb interaction in electron systems, similar mass enhancement may be observed for the orbital order transition because the orbital degrees may have anisotropic nature in the exchange process²¹⁾. It is conceivable that this mechanism of mass enhancement is relevant in the enhancement of the susceptibility χ and the specific heat coefficient γ for $(Y_{1-x}Ca_x)TiO_3$ near the metal-insulator transition point $x \sim 0.35$ which is far away from the Mott insulator at $x = 0$ ²²⁾. To judge the relevance of this proposal, it is desired to clarify experimentally whether the metal-insulator transition in $(Y_{1-x}Ca_x)TiO_3$ is accompanied by the orbital order transition.

The present study is a first step for a better understanding of the variety and universal aspects of transitions between the quantum liquid and the insulator beyond the statistics of particles. Several problems are left for further study. First, to put all the above discussions on more quantitative level, further detailed investigation is necessary. Especially, it is important to estimate the critical exponents in the transition to the component-ordered state. An interesting question is the relation of this transition at the incommensurate density to the novel universality class of the metal-insulator

transition characterized by the mass divergence at the commensurate density. The world-line algorithm which we have used is not efficient enough to give such quantitative details. An interesting approach for this purpose is to employ a model in which phase-separated region can be continuously reduced to the point, $\delta = 0$. This may help our further understanding of differences between the mass enhancement at the incommensurate density $n \neq 1$ and the commensurate density $n = 1$. In our calculations, δ_c decreases for the large value of V/t , although the phase-separated area remains finite. From the viewpoint of our numerical approach, large V/t yields an additional difficulty, that is, the acceptance ratio decreases in QMC updates, which leads to larger errorbars. Another possible way to reduce δ_c would be to include a component-exchange term, such as $J_{XY}\tilde{a}_{i,+}^\dagger\tilde{a}_{i,-}\tilde{a}_{j,-}^\dagger\tilde{a}_{j,+}$. At the present stage, it is difficult to include this process in the Monte Carlo study because of the sign problem.

§6. Summary

In this work, we have investigated the critical properties of various superfluid-insulator transitions in two dimensions. We have mainly considered the two-component lattice boson system with hard-core repulsion on a square lattice. The nearest neighbor interaction is taken component dependent. Our models exhibit two types of ordered states, the density order around $n = 1/2$ and the component order near $n = 1$. The Gutzwiller-type analysis shows uniform coexistence of the superfluidity and the density order near the density-ordered insulator at $n = 1/2$ for $V/t > 2$, whereas the phase separation with the Ising-type component order in one of the phases near $n = 1$. The transition from the superfluid to this phase separated state with the Ising-type ordering is a discontinuous one at the mean field level. The QMC study indicates several remarkable properties which are not predicted from the mean field results. The transition to the density-ordered phase as well as to the component-ordered phase is accompanied by phase separation. Moreover, in contradiction to the Gutzwiller results, all these transitions are continuous with the divergence of the correlation length of each order. This provides us with interesting examples of continuous phase transition which triggers phase separation. In spite of these similarities between the transitions to the density- and component-ordered phase, QMC results show qualitative differences between them. The most remarkable point is that the superfluid density ρ_s is severely reduced in the transition to the component-ordered state, whereas $\rho_s \neq 0$ in the phase-separated state with the density order. We have also investigated a single-component system which has the phase separation near the Mott insulator $n = 1$. There, ρ_s has a finite value at and around the transition. These results suggest that the superfluidity is suppressed by the component order of the Ising type but not by the orderings of the single-component origin. The second difference is seen in the correlation functions in each critical region of the density order transition and the component order transition. That is, the density correlation function exhibits only the commensurate peaks at $\vec{k} = \vec{Q}$, while the component correlation function has the incommensurate peaks when $V/t \neq 0$.

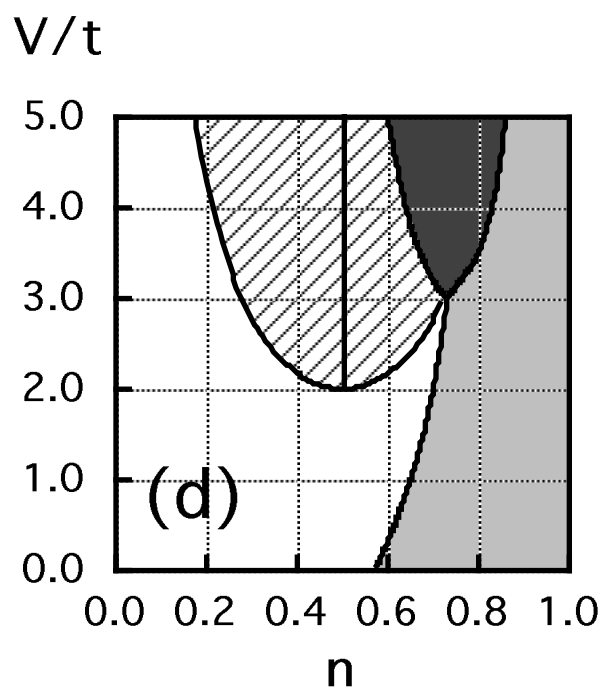
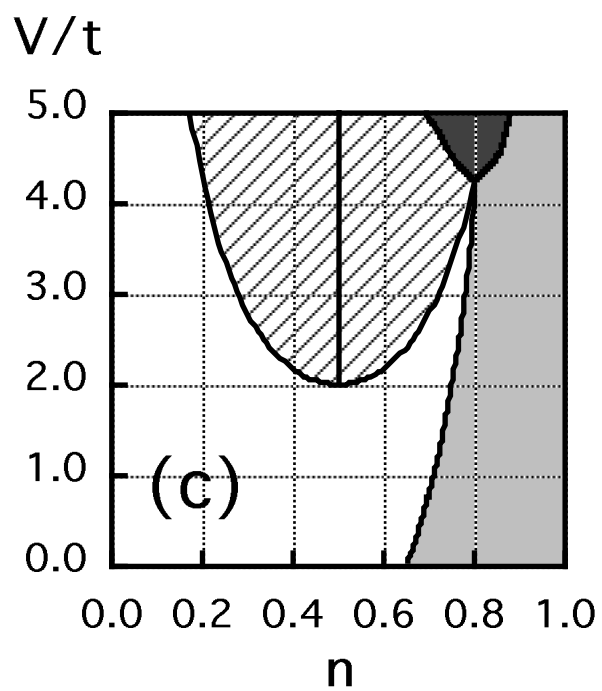
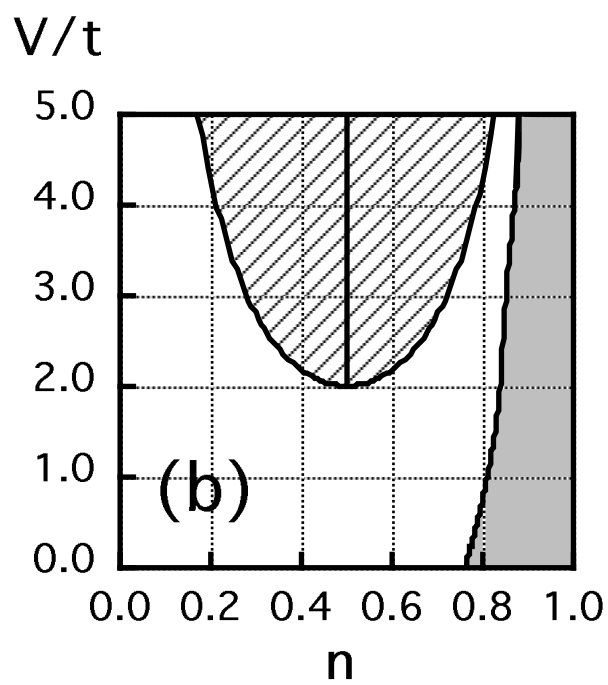
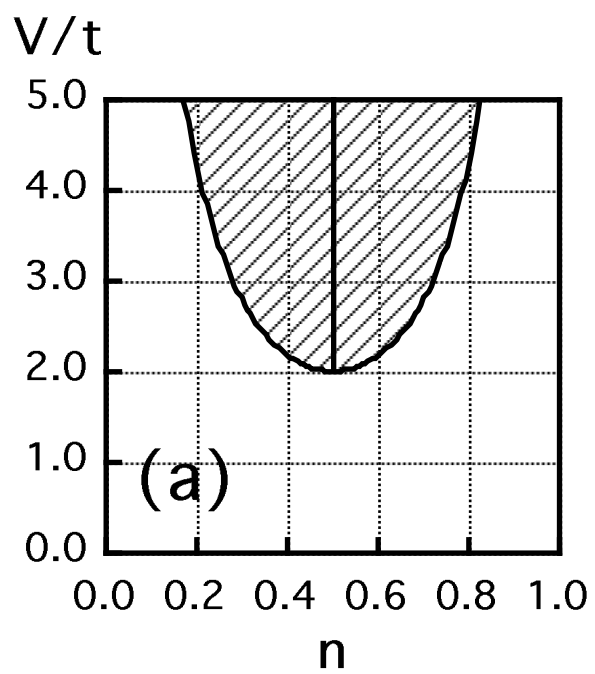
A remarkable consequence of our result is that there exists a mechanism of strong mass enhancement near the component order transition of the Ising type even when that transition takes place away from the commensurate density $n = 1$. The Ising exchange which presumably stabilizes the component order away from the commensurate density $n = 1$ also causes the mass enhancement. We have proposed a picture of the hole trapping under the Ising ordering as the origin of this type of mass enhancement. The present mechanism of the mass enhancement is different from the mass divergence at the commensurate density clarified in the two-dimensional Hubbard model. Detailed comparison between these two types of singularities is left for further study. We have also discussed a possible relevance of this type of mass enhancement to the metal-insulator transition of $(Y_{1-x}Ca_x)TiO_3$ at the incommensurate density $x \sim 0.35$. In this scenario, the orbital order is stabilized by the Ising-type stabilization mechanism at densities away from the filling of the Mott insulator and this mechanism also induces the mass enhancement as well as the metal-insulator transition itself if combined with finite disorder. Detailed analysis on a quantitative level on a microscopic model remains for further studies.

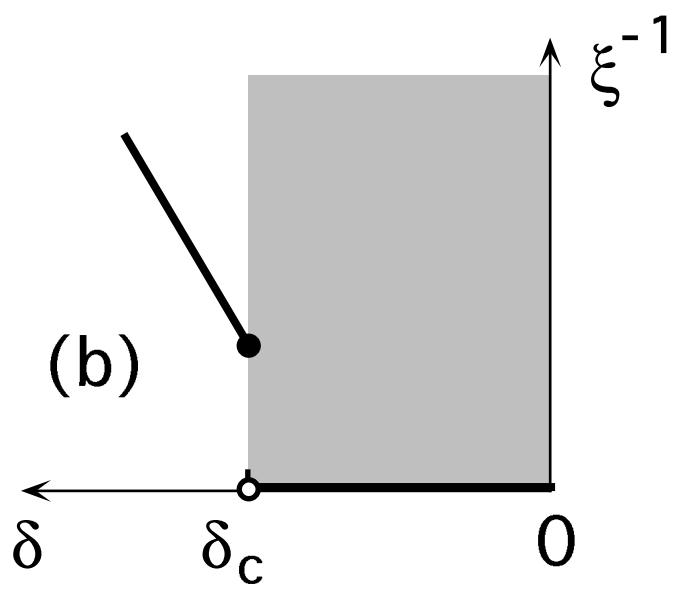
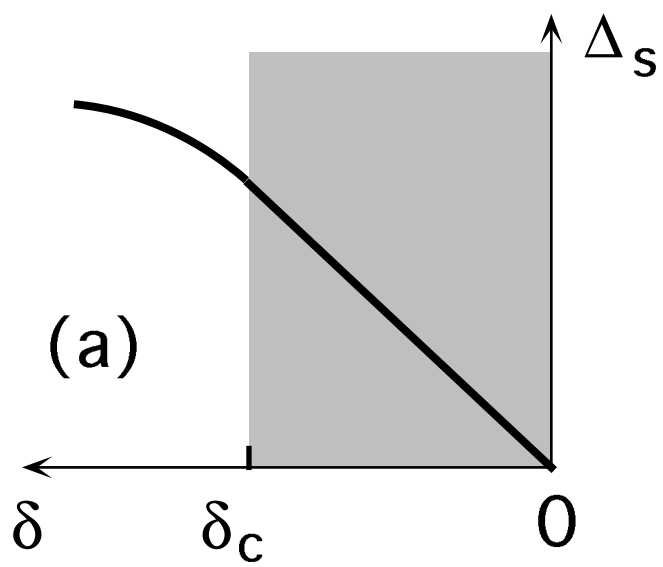
Acknowledgement

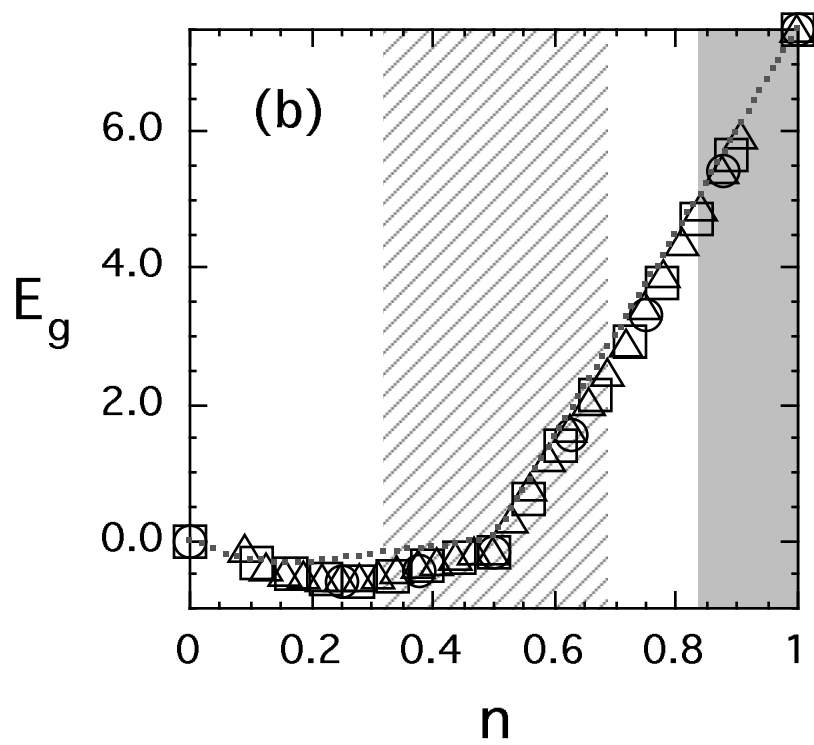
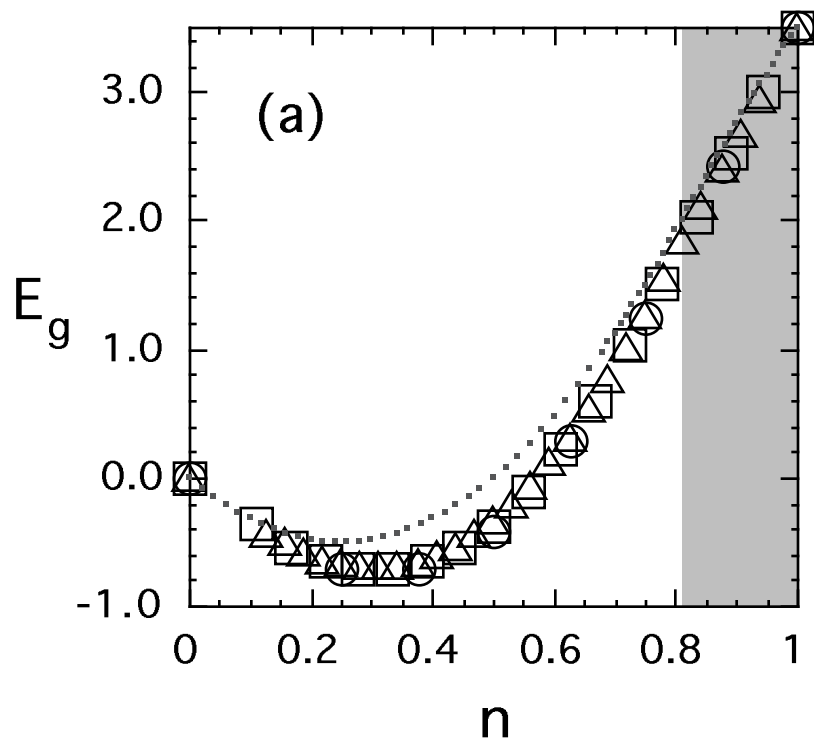
This work is supported by a Grant-in-Aid for Scientific Research on the Priority Area 'Anomalous Metallic State near the Mott Transition' from the Ministry of Education, Science and Culture, Japan.

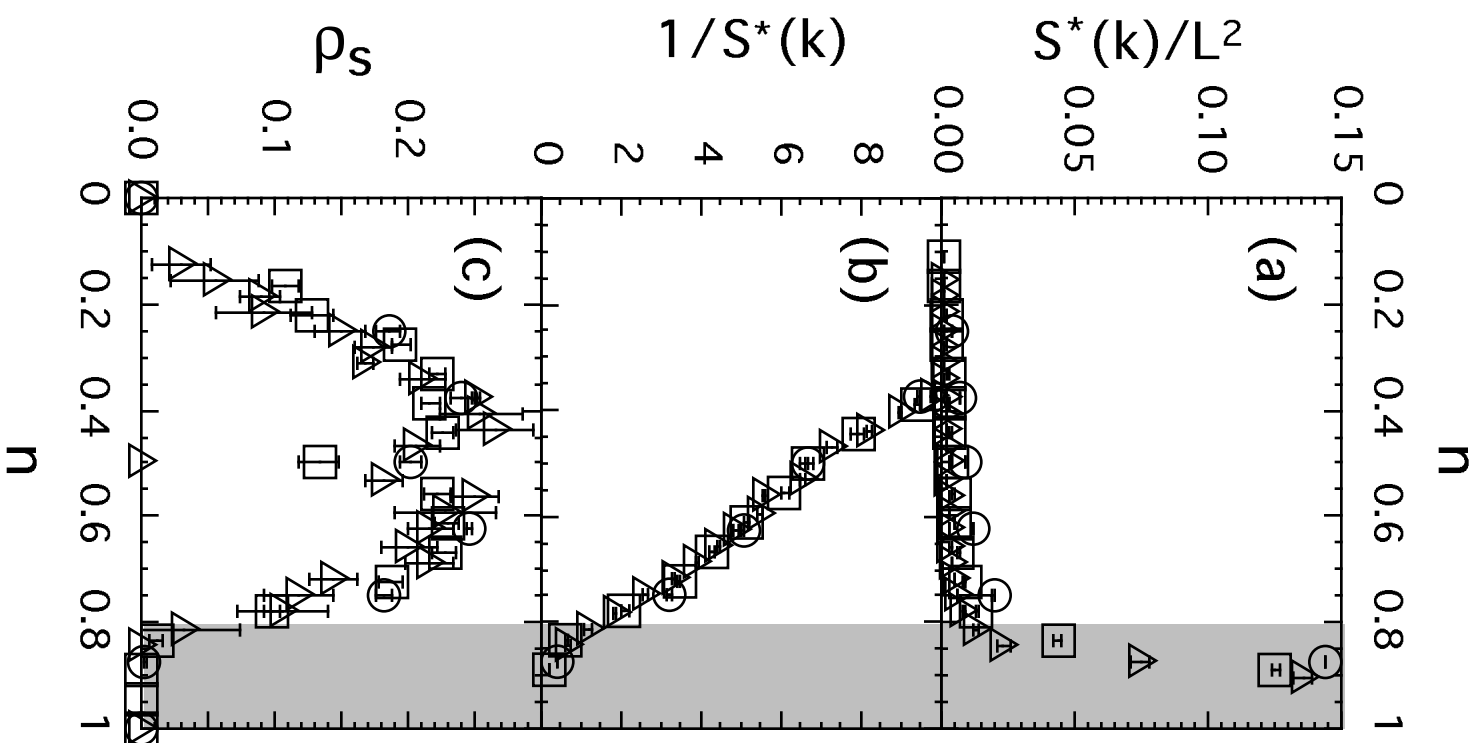
-
- [1] M. Imada : J. Phys. Soc. Jpn. **64** (1995) 2956.
 - [2] N. Furukawa and M. Imada : J. Phys. Soc. Jpn. **61** (1992) 3331.
 - [3] F. F. Assaad and M. Imada : submitted to Phys. Rev. Lett.
 - [4] M. P. A. Fisher, P. B. Weichman, G. Grinstein and D. S. Fisher : Phys. Rev. B **40** (1989) 546.
 - [5] G. G. Batrouni, R. T. Scalettar and G. T. Zimanyi : Phys. Rev. Lett. **65** (1990) 1765; G. G. Batrouni, R. T. Scalettar and G. T. Zimanyi : Phys. Rev. B **46** (1992) 9051.
 - [6] W. Krauth and N. Trivedi : Europhys. Lett. **14** (1991) 627.
 - [7] M. Imada : J. Phys. Soc. Jpn. **63** (1994) 3059.
 - [8] T. Onogi and Y. Murayama : Phys. Rev. B **49** (1994) 9009.
 - [9] G. G. Batrouni, R. T. Scalettar, G. T. Zimanyi and A. P. Kampf : Phys. Rev. Lett. **74** (1995) 2527; R. T. Scalettar, G. G. Batrouni, A. P. Kampf and G. T. Zimanyi : Phys. Rev. B **51** (1995) 8467.
 - [10] M. C. Gutzwiller : Phys. Rev. **134** (1964) A923.
 - [11] D. S. Rokhsar and K. G. Kotliar : Phys. Rev. B **44** (1991) 10328.
 - [12] D. Vollhardt : Rev. Mod. Phys. **56** (1985) 99 and references there in.
 - [13] H. Yokoyama and H. Shiba : J. Phys. Soc. Jpn. **56** (1987) 1490.
 - [14] M. S. Makivić and H. -Q. Ding : Phys. Rev. B **43** (1991) 3562.
 - [15] E. L. Pollock and D. M. Ceperley : Phys. Rev. B **36** (1987) 8343.

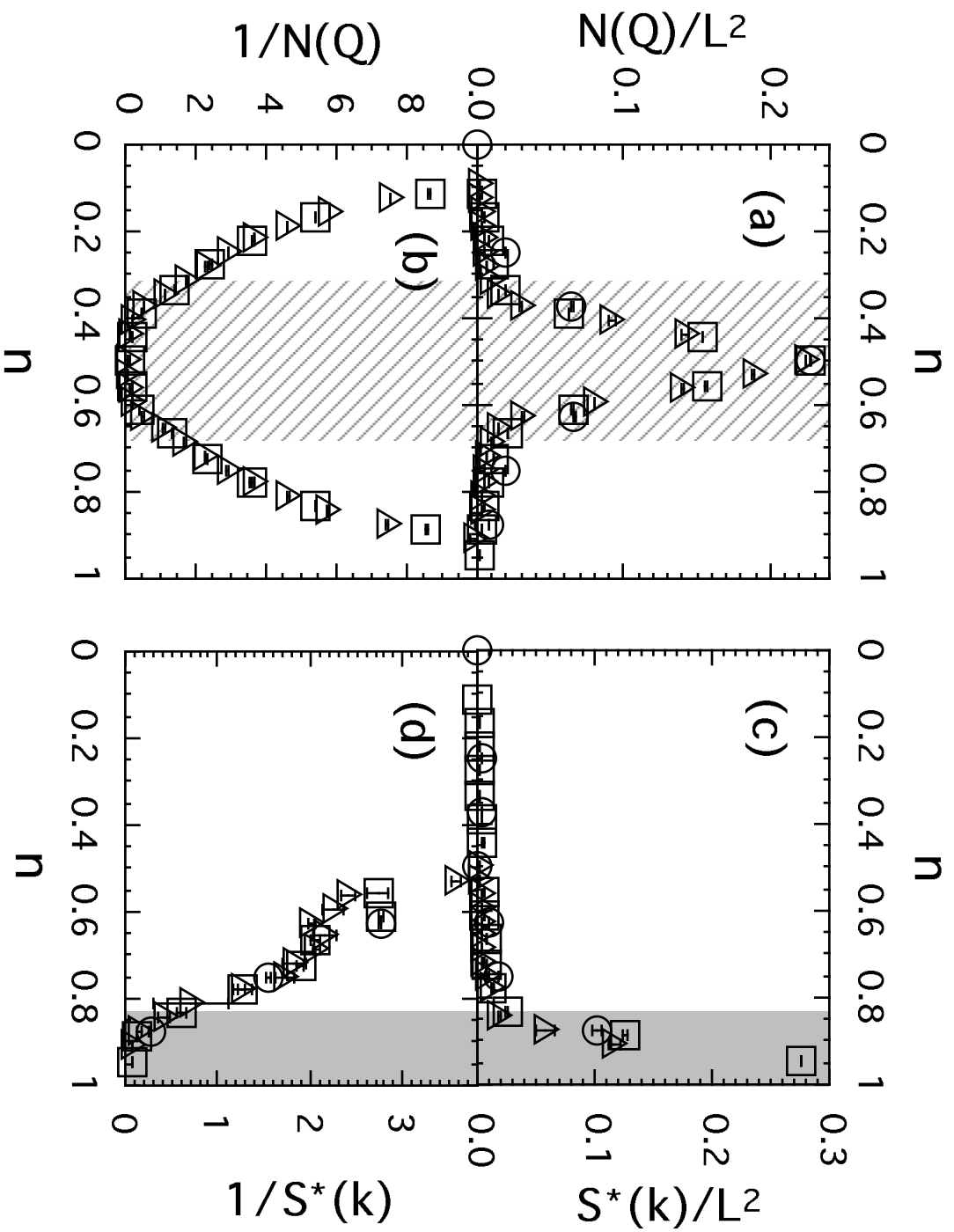
- [16] This temperature is not low enough to investigate the component order in the density-ordered state. We comment this point in §4.2.
- [17] In the classical consideration, however, the ground state has macroscopic degrees of degeneracy due to strong frustration of the nearest neighbor and the next nearest neighbor couplings.
- [18] M. Imada : J. Phys. Soc. Jpn. **62** (1993) 1105.
- [19] C. L. Kane, P. A. Lee and N. Read : Phys. Rev. B **39** (1989) 6880.
- [20] D. Poilblanc, T. Ziman and E. Dagotto : Phys. Rev. B **47** (1993) 14267.
- [21] K.I.Kugel' and D.I.Khomskii : Usp.Fiz.Nauk. **136** (1982) 621, [Sov.Phys.Usp. **25** (1982) 231] and references there in.
- [22] K. Kumagai, T Suzuki, Y. Taguchi, Y. Okada, Y. Fujishima and Y. Tokura : Phys. Rev. B **48** (1993) 7636.

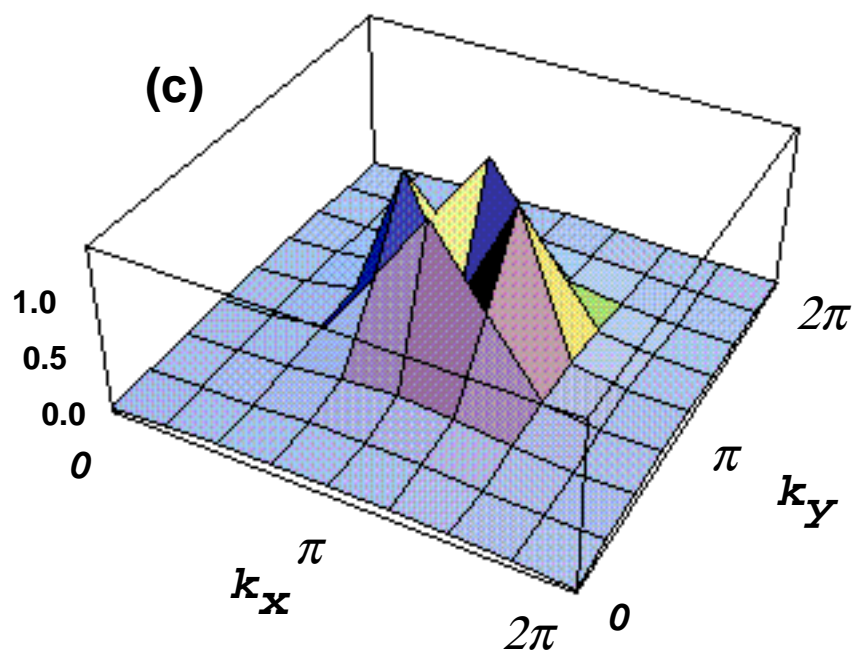
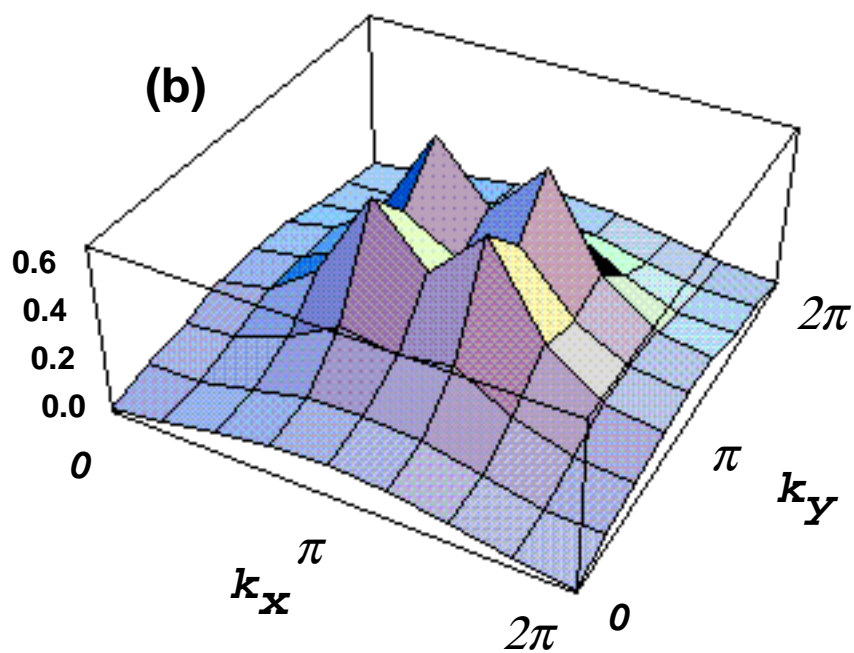
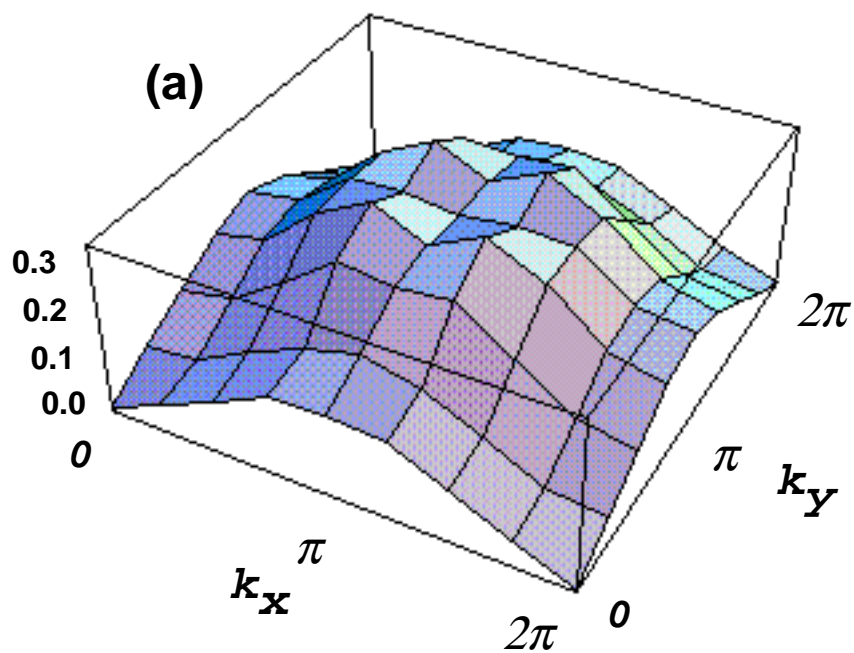


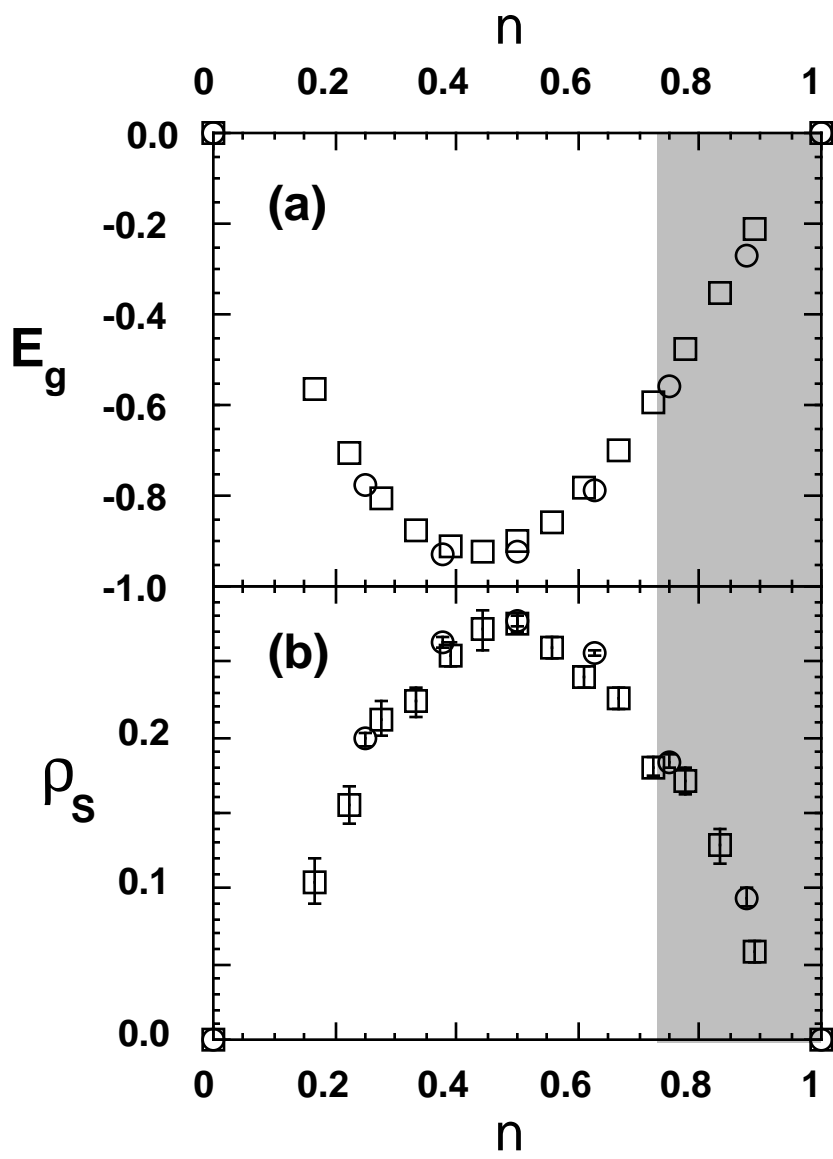


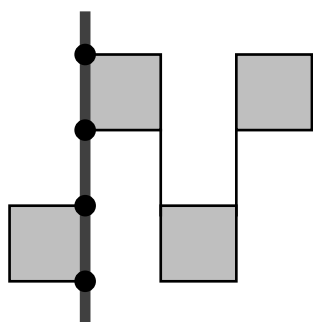




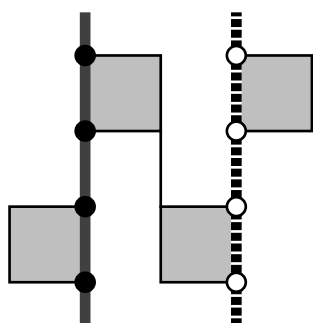
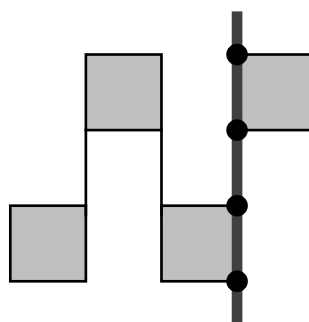




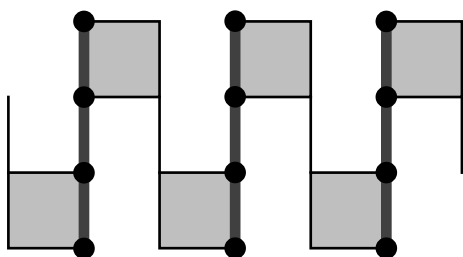
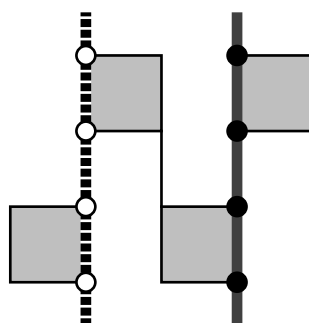




(a)



(b)



(c)

